

# Investigation of cerebellar damage in adult amyotrophic lateral sclerosis patients using magnetic resonance imaging and diffusion tensor imaging

Marta Nowakowska-Kotas<sup>1,A–F</sup>, Adrian Korbecki<sup>2,B–D,F</sup>, Sławomir Budrewicz<sup>1,C,E,F</sup>, Joanna Bładowska<sup>3,A,C,E,F</sup>

<sup>1</sup> Department of Neurology, Wrocław Medical University, Poland

<sup>2</sup> Chair of Radiology, Department of General Radiology, Interventional Radiology and Neuroradiology, Wrocław Medical University, Poland

<sup>3</sup> Department of Radiology, 4<sup>th</sup> Military Clinical Hospital, Wrocław, Poland

A – research concept and design; B – collection and/or assembly of data; C – data analysis and interpretation;

D – writing the article; E – critical revision of the article; F – final approval of the article

Advances in Clinical and Experimental Medicine, ISSN 1899–5276 (print), ISSN 2451–2680 (online)

*Adv Clin Exp Med.* 2024;33(9):1023–1028

## Address for correspondence

Marta Nowakowska-Kotas

E-mail: marta.nowakowska-kotas@umw.edu.pl

## Funding sources

None declared

## Conflict of interest

None declared

Received on March 26, 2023

Reviewed on May 12, 2023

Accepted on September 21, 2023

Published online on November 14, 2023

## Cite as

Nowakowska-Kotas M, Korbecki A, Budrewicz S, Bładowska J. Investigation of cerebellar damage in adult amyotrophic lateral sclerosis patients using magnetic resonance imaging and diffusion tensor imaging. *Adv Clin Exp Med.* 2024;33(9):1023–1028. doi:10.17219/acem/172698

## DOI

10.17219/acem/172698

## Copyright

Copyright by Author(s)

This is an article distributed under the terms of the Creative Commons Attribution 3.0 Unported (CC BY 3.0) (<https://creativecommons.org/licenses/by/3.0/>)

## Abstract

**Background.** Research on amyotrophic lateral sclerosis (ALS) reveals that the disorder is not restricted to motor neurons.

**Objectives.** This neuroimaging study aimed to investigate the presence of cerebellar damage in adult ALS patients.

**Materials and methods.** The study retrospectively analyzed magnetic resonance imaging (MRI) examinations performed on a 1.5T MR unit of 33 patients (17 men and 16 women with a mean age of 59.3 years) diagnosed with ALS. Cerebellar and posterior fossa dimensions were calculated using plain MR images. In addition, diffusion tensor imaging (DTI) was used to obtain white matter integrity measurements, represented as fractional anisotropy (FA) values, in the posterior limbs of internal capsules (PLIC) and middle cerebellar peduncles (MCPs). These measurements were compared to 36 healthy volunteers (11 men and 25 women with a mean age of 55.3 years). The study also assessed clinical data for correlations with cerebellar imaging findings.

**Results.** The linear measurements of the cerebellum did not differ between groups. However, the transverse cerebellar dimension (TCD) ratio to the maximum length of the posterior fossa (0.973 compared to 0.982,  $t = -2.76$ ,  $p < 0.01$ ) and FA value in both MCPs (0.67 compared to 0.65 and 0.69 compared to 0.67,  $p < 0.05$ ) were significantly lower in ALS patients. No significant differences were found in FA value in the PLIC, and no significant correlations were observed between patient clinical characteristics and cerebellar damage.

**Conclusions.** This study provides evidence of cerebellar damage in adult ALS patients. These findings contribute to ALS understanding and highlight the importance of considering cerebellar involvement in the disease process. The results suggest that measuring the TCD ratio and FA value in both MCPs could be potential biomarkers for cerebellar damage in ALS patients.

**Key words:** cerebellum, magnetic resonance imaging, amyotrophic lateral sclerosis, fractional anisotropy, transverse cerebellar diameter

## Background

Amyotrophic lateral sclerosis (ALS) affects both upper and lower motor neurons. Some non-motor symptoms may also be present, including extrapyramidal symptoms,<sup>1</sup> cerebellar signs<sup>2</sup> and dementia.<sup>3,4</sup> This condition is characterized by the loss of cortical motor neurons and cortical atrophy of the motor cortex,<sup>5</sup> leading to motor preparation and initiation difficulties. Compensation mechanisms are then activated in the premotor area, cerebellum and basal ganglia.<sup>6–8</sup>

The cerebellum plays a crucial role in ALS, extending beyond motor control to various cognitive processes such as working memory, verbal fluency and emotion-affect control.<sup>9,10</sup> Imaging studies have shown inconsistent data on cerebellar changes in ALS, with atrophy of the whole cerebellum, focal changes in specific lobules, changes in the integrity of cerebellar peduncles, and increased metabolism in various cerebellar regions being reported.<sup>2,11–15</sup> Advanced magnetic resonance imaging (MRI) techniques, such as diffusion tensor imaging (DTI), enable the measurement of anisotropic diffusion of water molecules within tissue. By calculating the fractional anisotropy (FA) parameter, characteristic changes in brain tissues at the level of cellular microarchitecture can be depicted, as well as changes in apparently normal white matter that are not visible on conventional MRI.<sup>16</sup>

## Objectives

The objective of this investigation was to ascertain the linear dimensions of the cerebellum and the posterior cranial fossa, and assess the association between these parameters and white matter integrity, gender, disease duration, and age in patients with ALS compared to healthy controls.

## Materials and methods

This investigation employed a retrospective case-control design, utilizing standard diagnostic data documented in all patients diagnosed with ALS at the Department of Neurology of the University Clinical Hospital (Wrocław, Poland). The MRI examinations were conducted at the Department of Radiology of the same hospital. All participants provided informed consent. The approval of the local Bioethics Committee of Wrocław Medical University was obtained (approval No. 885/2022).

### The study group

The study group consisted of 33 subsequent patients (16 women and 17 men with a mean age of 59.3 years, standard deviation (SD)  $\pm 11.2$  years) from the Department of Neurology, diagnosed with ALS between 2017 and 2018 based on the El Escorial criteria.<sup>17</sup> Disease-related variables (type and duration of the disease and first symptoms)

were established based on medical records. The mean time of disease duration until the MRI examination was noted as 1.43 years (median: 1 year, range: 0.5–4 years).

Exclusion criteria included cerebrovascular events, neoplasm or paraneoplastic syndromes in a patient's medical history, present overt dementia, or extrapyramidal and cerebellar signs in the neurological examination.

### Magnetic resonance imaging protocol

The MRI examinations for ALS patients and controls were conducted using a Signa HDx 1.5 Tesla MRI unit (GE Medical Systems, Chicago, USA) and a 16-channel head and spine (HNS) coil. A conventional brain MRI protocol was initially performed with the following sequences: sagittal and coronal T2 fast recovery spin echo (FRFSE), axial T1 spin echo (SE), axial T2 fast spin-echo (FSE), axial fluid-attenuated inversion recovery (FLAIR), axial diffusion-weighted imaging (DWI) SE-echo-planar imaging (EPI) sequences, and a gadolinium-enhanced three-dimensional-fast spoiled gradient-echo (3D-FSPGR) T1 sequence. Subsequently, linear measurements of the cerebellum were obtained from axial and sagittal T2-FSE sequences (Fig. 1). The transverse cerebellar diameter (TCD) and the maximum length of the posterior fossa were measured twice. To standardize the TCD to the head size, the ratio between 2 parameters (TCD and the maximum width of the posterior cranial fossa) was calculated and used as the fundamental parameter for further analyses.

### Diffusion tensor imaging

Diffusion tensor imaging (DTI) examinations were performed using a single-shot (SS) EPI sequence in 25 different diffusion-encoding directions, with the following parameters: b-values = 0 and 1000 s/mm<sup>2</sup>, transfer ratio (TR) = 8500 ms, time to echo (TE) = 100 ms, field of view (FOV) = 24 × 24 cm, and a matrix = 128 × 128 mm, with 2.5 mm-thick axial slices obtained parallel to the anterior and posterior commissures. The DTI data were post-processed on the Advantage Workstation 4.6 (GE Medical Systems) using Ready View software provided by the manufacturer. The FA values were evaluated bilaterally in the following white matter tracts: posterior limbs of internal capsules (PLIC) and middle cerebellar peduncles (MCP) in small, fixed-in-size and circular regions of interest (ROIs; size 25–30 mm<sup>2</sup>) were assessed by means of color-coded maps. The mean FA values out of 3 measurements were calculated.

### The control group

Thirty-six healthy age-matched controls (25 women and 11 men with a mean age of 55.4  $\pm$  15.9 years) were recruited (volunteers, mainly hospital staff members) to obtain normal values for neuroimaging measurements.

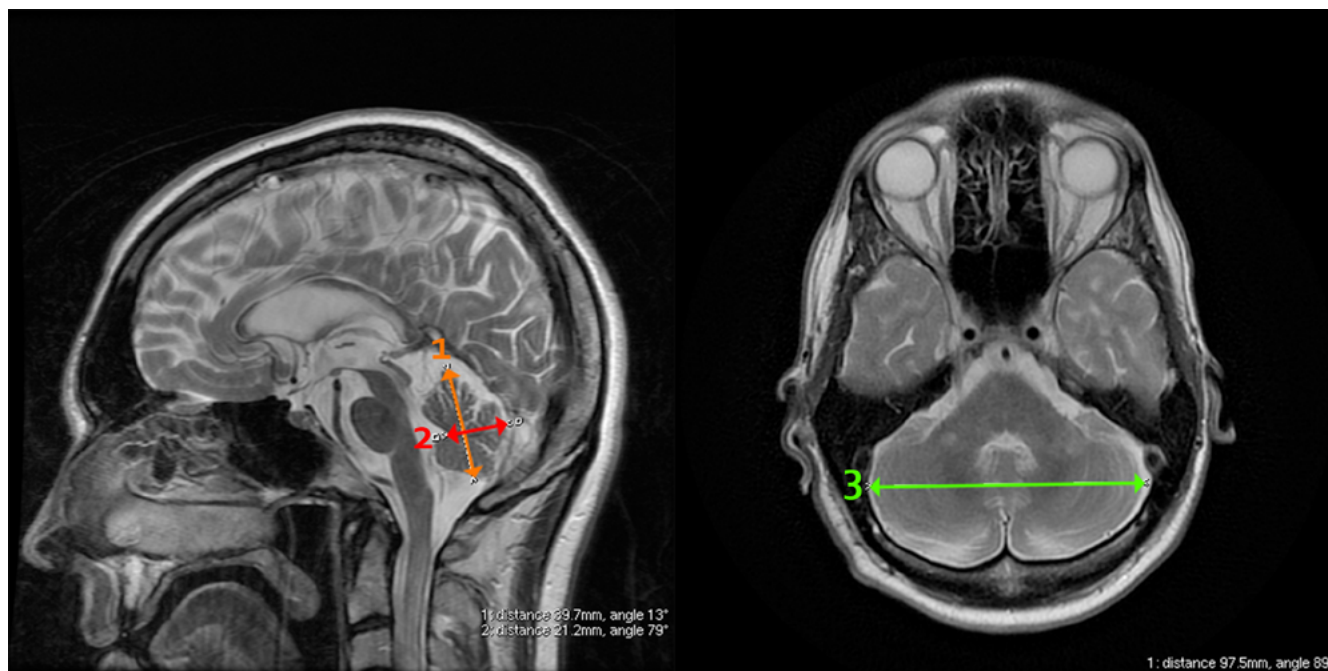


Fig. 1. Cerebellum linear measurements on T2-weighted sagittal and axial plains cerebellum height (1 – orange arrow), cerebellum width (2 – red arrow) and transverse cerebellar diameter (3 – green arrow).

### Clinical–neuroimaging correlations

Measurements of the cerebellum and posterior fossa and DTI parameters were compared between patient and control groups. The ALS characteristics (onset of symptoms and disease duration) and the abovementioned variables were analyzed to identify potential correlations with cerebellar dimensions.

### Statistical analyses

Statistical analyses employed STATISTICA PL v. 8 software (StatSoft Polska, Cracow, Poland). A p-value <0.05 was considered statistically significant. The normality of distribution for all continuous variables was verified with a Shapiro–Wilk test to select appropriate statistical methods. Comparisons between 2 independent groups were performed using Student’s t-test and the Mann–Whitney U test (Supplementary Table 1). A Kruskal–Wallis

analysis of variance (ANOVA) rank test compared categorical independent variables. Pearson’s correlation was used to assess clinical–radiological correlations.

### Results

The measurements of the cerebellum in both groups are presented in Table 1. Although the posterior fossa dimension and transcerebellar diameter did not differ statistically, the calculated ratio (TCD/posterior fossa dimension) revealed a significant difference between ALS patients and controls (median: 0.978 compared to 0.984, U = 845.0, p = 0.002). The dimensions of the posterior fossa and TCD differed between male and female patients (107.7 mm compared to 103.3 mm, p < 0.005, and 104.5 mm compared to 100.8 mm, p < 0.01, respectively). The TCD showed a significant correlation with age (r = –0.38, p < 0.05). The ratio of the TCD/posterior

Table 1. Basic characteristics of the cerebellar linear measurements in patient and control groups

Parameter	Patients (n = 33)			Controls (n = 36)			p-value (used test)
	mean [mm]	median [mm]	95% CI/Q1–Q3	mean [mm]	median [mm]	95% CI/Q1–Q3	
Posterior fossa dimension	105.5	105.3	103.99; 107.07	106.5	105.5	105.1; 108.0	0.33 (Student’s t)
Transcerebellar diameter (TCD)	102.7	103.0	101.3; 104.2	104.4	104.8	103.0; 105.8	0.1 (Student’s t)
Cerebellar width	46.4	47.0	45.2; 47.2	46.4	46.7	45.5; 47.3	0.95 (Student’s t)
Cerebellar height	25.8	25.1	23.9–26.9	26.0	26.2	23.9–27.9	0.42 (Mann–Whitney U)

95% CI – 95% confidence interval; Q1 – 1<sup>st</sup> quartile; Q3 – 3<sup>rd</sup> quartile; TCD – transverse cerebellar dimension.

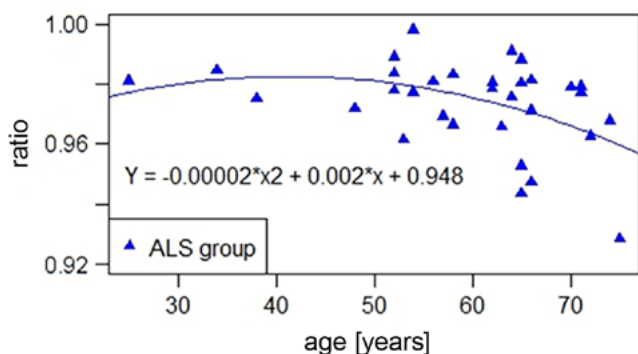


Fig. 2. Correlation of the ratio of transverse cerebellar dimension (TCD) measurements to the posterior fossa dimension in relation to age in amyotrophic lateral sclerosis (ALS) patients

fossa dimension significantly correlated with the age of the patients ( $S = -0.370$ ,  $p < 0.05$ ) (Fig. 2). Analysis of the correlation between age and TCD/posterior fossa ratio was significant only in the ALS group. As the ratio of the TCD/posterior fossa dimension did not have a normal distribution in either group, a Spearman's rank correlation test was used. In the control group, the rho value was  $-0.324$ , corresponding to a p-value of 0.053, slightly above the assumed significance level of 0.05. In the ALS group, Spearman's rank correlation rho was  $-0.370$ , corresponding to a p-value of 0.034. A series of fitting several polynomial regression models, from 1 up to 5 degrees, were conducted to assess the nature of the relationship. The calculated adjusted  $R^2$  of each model was the highest for the second-degree polynomial, which had an adjusted  $R^2$  of 0.132. The p-value for the selected model as a whole was 0.046. The coefficient estimates and 95% confidence intervals (95% CIs) are presented in Supplementary Table 2. No other correlations for cerebellar linear measurements and sex, age or duration of the disease and its first symptoms were found.

The FA values were significantly different between controls and patients in both MCPs but not at the level of the internal capsules (Table 2). Strong correlations were found between FA values in the PLIC on both sides ( $S = 0.49$ ,  $p < 0.005$  (Spearman's correlation)) and FA in MCP on both sides. No correlation was found between linear cerebellum measurements and FA values in ALS patients.

## Discussion

The method used in this study (i.e., linear measurements were easily performed on axial and sagittal T2-FSE) proved simple, effective and feasible for all subjects. The TCD alone showed sexual dimorphism, a typical observation during the developmental period but not uniformly found in mature brains.<sup>18,19</sup> In turn, the TCD/posterior fossa dimension ratio had a nonlinear correlation with age in healthy and patient groups. Since TCD correlated significantly with age, a change in the ratio occurred due to atrophy of the cerebellum, which has also been described by other authors using both linear and volumetric measurements.<sup>20–23</sup>

The TCD/posterior fossa ratio decreased with age significantly faster in patients than in controls, which would be consistent with observations of most authors describing the decrease in the cerebellum or individual cerebellar lobes and brainstem size or volume, with the degree of atrophy varying according to the form of motor neuron disease, the severity of motor disturbances, and the presence of behavioral and cognitive dysfunctions.<sup>24–27</sup> In contrast, some authors report no significant abnormalities in cerebellar volumetric measurements.<sup>28,29</sup> Several factors contribute to the variability of our findings, with emerging evidence that genetic and sporadic ALS differ in their imaging signature.<sup>2,13</sup> There is a significant association between cerebellar atrophy in ALS combined with frontotemporal dementia (FTD) or carrying C9orf72 hexanucleotide repeat expansion in patients who already show some cognitive impairment (ALSci), as opposed to patients presenting with more behavioral abnormalities (ALSbi).<sup>13,30,31</sup> Patients with ALS-ataxia continuum symptoms do not display such abnormalities.<sup>13</sup>

The various patterns of white matter integrity change observed using DTI in ALS patients need to be emphasized because they may offer unique insights into the neurodegeneration processes and ALS pathophysiology. The measurements of FA values in the PLIC and MCP, which include the corticopontocerebellar pathway, showed significant differences between patients and healthy controls in the MCP but not at the level of the PLIC. Other authors have demonstrated a significantly decreased FA value at the pyramidal pathways and, in some cases, at the MCP

Table 2. Diffusion tensor imaging (DTI) measurements of fractional anisotropy (FA) on both sides of posterior limbs of internal capsules (PLIC) and middle cerebellar peduncles (MCP) in patients and controls

Region	Patients (n = 33)			Controls (n = 36)			p-value (used test)
	mean FA	median	95% CI/Q1–Q3	mean FA	median	95% CI/Q1–Q3	
MCP right	0.67	0.68	0.66; 0.69	0.65	0.64	0.64; 0.66	<0.001 (Student's t)
MCP left	0.69	0.69	0.67; 0.71	0.67	0.67	0.66; 0.68	0.052 (Welch's t)
PLIC right	0.62	0.62	0.61; 0.63	0.63	0.63	0.62; 0.64	0.23 (Student's t)
PLIC left	0.64	0.63	0.62; 0.65	0.64	0.64	0.62; 0.66	0.29 (Mann–Whitney U)

95% CI – 95% confidence interval; Q1 – 1<sup>st</sup> quartile; Q3 – 3<sup>rd</sup> quartile.

level.<sup>32–38</sup> Our findings, together with the atrophy phenomenon discussed earlier, suggest the simultaneous occurrence of cerebellar degeneration and loss of the integrity of pathways connecting this structure with other brain regions. Our study also indicates that this process occurs at a different rate and somewhat independently of pyramidal tract degeneration, consistent with coexisting degenerative and compensatory processes postulated in other papers.<sup>6,8,39</sup> This alternation of cerebrocerebellar connectivity<sup>8,28,36,40–42</sup> underscores the importance of understanding the complex and multifactorial nature of ALS pathology.

## Limitations

Although our results are easily accessible and encouraging, the study had some limitations. First, the retrospective design and relatively small number of patients included in our study limited the number of examination techniques. Second, the patients could have diverse clinical phenotypes and severity levels of the disease, which may have resulted in various predispositions to cerebellar abnormalities.<sup>13,43,44</sup> Third, the measurements were done using certified software provided by the MRI manufacturer, reducing the potential number of measurements to those that are relatively simple. Despite these limitations, our study provides important insights into the specific patterns of cerebellar damage in ALS patients. Our method was simple and can be improved in further longitudinal projects.

## Conclusions

This study shows that a simple MRI measurement might reveal accelerated cerebellar atrophy in ALS patients, which correlates with reduced white matter integrity in the cerebellar afferent pathways. Our results highlight the importance of cerebellar pathology in these patients.

## Supplementary data

The Supplementary materials are available at <https://doi.org/10.5281/zenodo.8321084>. The package consists of the following files:


Supplementary Table 1. Normality and variance tests.


Supplementary Table 2. Coefficient estimates together with 95% CI for polynomial regression models of correlation of the age and ratio of the TCD to the dimension of the posterior fossa.

## ORCID iDs

Marta Nowakowska-Kotas  <https://orcid.org/0000-0002-3173-8337>

Adrian Korbecki  <https://orcid.org/0000-0003-0047-9819>

Sławomir Budrewicz  <https://orcid.org/0000-0002-2044-6347>

Joanna Bladowska  <https://orcid.org/0000-0003-0597-8457>

## References

- Pradat PF, Bruneteau G, Munerati E, et al. Extrapyramidal stiffness in patients with amyotrophic lateral sclerosis. *Mov Disord*. 2009;24(14):2143–2148. doi:10.1002/mds.22762
- Prell T, Grosskreutz J. The involvement of the cerebellum in amyotrophic lateral sclerosis. *Amyotroph Lateral Scler Frontotemporal Degener*. 2013;14(7–8):507–515. doi:10.3109/21678421.2013.812661
- Mackenzie IRA, Frick P, Neumann M. The neuropathology associated with repeat expansions in the *C9ORF72* gene. *Acta Neuropathol*. 2014;127(3):347–357. doi:10.1007/s00401-013-1232-4
- Strong MJ, Abrahams S, Goldstein LH, et al. Amyotrophic lateral sclerosis-frontotemporal spectrum disorder (ALS-FTSD): Revised diagnostic criteria. *Amyotroph Lateral Scler Frontotemporal Degener*. 2017;18(3–4):153–174. doi:10.1080/21678421.2016.1267768
- Bede P, Bokde A, Elamin M, et al. Grey matter correlates of clinical variables in amyotrophic lateral sclerosis (ALS): A neuroimaging study of ALS motor phenotype heterogeneity and cortical focality. *J Neurol Neurosurg Psychiatry*. 2013;84(7):766–773. doi:10.1136/jnnp-2012-302674
- Proudfoot M, Bede P, Turner MR. Imaging cerebral activity in amyotrophic lateral sclerosis. *Front Neurol*. 2019;9:1148. doi:10.3389/fneur.2018.01148
- Mohammadi B, Kollwe K, Cole DM, et al. Amyotrophic lateral sclerosis affects cortical and subcortical activity underlying motor inhibition and action monitoring. *Hum Brain Mapp*. 2015;36(8):2878–2889. doi:10.1002/hbm.22814
- Abidi M, De Marco G, Couillandre A, et al. Adaptive functional reorganization in amyotrophic lateral sclerosis: Coexisting degenerative and compensatory changes. *Eur J Neurol*. 2020;27(1):121–128. doi:10.1111/ene.14042
- Argyropoulos GPD, Van Dun K, Adamaszek M, et al. The cerebellar cognitive affective/Schmahmann syndrome: A Task Force paper. *Cerebellum*. 2020;19(1):102–125. doi:10.1007/s12311-019-01068-8
- Kozioł LF, Budding D, Andreasen N, et al. Consensus paper: The cerebellum's role in movement and cognition. *Cerebellum*. 2014;13(1):151–177. doi:10.1007/s12311-013-0511-x
- Christidi F, Karavasilis E, Riederer F, et al. Gray matter and white matter changes in non-demented amyotrophic lateral sclerosis patients with or without cognitive impairment: A combined voxel-based morphometry and tract-based spatial statistics whole-brain analysis. *Brain Imaging Behav*. 2018;12(2):547–563. doi:10.1007/s11682-017-9722-y
- Cistaro A, Valentini MC, Chiò A, et al. Brain hypermetabolism in amyotrophic lateral sclerosis: A FDG PET study in ALS of spinal and bulbar onset. *Eur J Nucl Med Mol Imaging*. 2012;39(2):251–259. doi:10.1007/s00259-011-1979-6
- Bede P, Chipika RH, Christidi F, et al. Genotype-associated cerebellar profiles in ALS: Focal cerebellar pathology and cerebro-cerebellar connectivity alterations. *J Neurol Neurosurg Psychiatry*. 2021;92(11):1197–1205. doi:10.1136/jnnp-2021-326854
- Prudlo J, Bißbort C, Glass A, et al. White matter pathology in ALS and lower motor neuron ALS variants: A diffusion tensor imaging study using tract-based spatial statistics. *J Neurol*. 2012;259(9):1848–1859. doi:10.1007/s00415-012-6420-y
- Trojsi F, Di Nardo F, D'Alvano G, et al. Resting state fMRI analysis of pseudobulbar affect in amyotrophic lateral sclerosis (ALS): Motor dysfunction of emotional expression. *Brain Imaging Behav*. 2023;17(1):77–89. doi:10.1007/s11682-022-00744-4
- Bladowska J, Zimny A, Kołtowska A, et al. Evaluation of metabolic changes within the normal appearing gray and white matters in neurologically asymptomatic HIV-1-positive and HCV-positive patients: Magnetic resonance spectroscopy and immunologic correlation. *Eur J Radiol*. 2013;82(4):686–692. doi:10.1016/j.ejrad.2012.11.029
- Brooks BR, Miller RG, Swash M, Munsat TL. El Escorial revisited: Revised criteria for the diagnosis of amyotrophic lateral sclerosis. *Amyotroph Lateral Scler Other Motor Neuron Disord*. 2000;1(5):293–299. doi:10.1080/146608200300079536
- Imamoglu EY, Gursoy T, Ovali F, Hayran M, Karatekin G. Nomograms of cerebellar vermis height and transverse cerebellar diameter in appropriate-for-gestational-age neonates. *Early Hum Dev*. 2013;89(12):919–923. doi:10.1016/j.earlhumdev.2013.10.001
- Co E, Raju TN, Aldana O. Cerebellar dimensions in assessment of gestational age in neonates. *Radiology*. 1991;181(2):581–585. doi:10.1148/radiology.181.2.1924808

20. Captier G, Boë LJ, Badin P, Guihard-Costa AM, Canovas F, Larroche JC. Modèles géométriques de croissance du cerveau, cervelet, tronc cérébral et modification des angles de la base du crâne au cours de la période fœtale. *Morphologie*. 2013;97(317):38–47. doi:10.1016/j.morpho.2012.12.002
21. Luft AR. Patterns of age-related shrinkage in cerebellum and brainstem observed in vivo using three-dimensional MRI volumetry. *Cereb Cortex*. 1999;9(7):712–721. doi:10.1093/cercor/9.7.712
22. Raz N, Schmiedek F, Rodrigue KM, Kennedy KM, Lindenberger U, Lövdén M. Differential brain shrinkage over 6 months shows limited association with cognitive practice. *Brain Cogn*. 2013;82(2):171–180. doi:10.1016/j.bandc.2013.04.002
23. Han S, An Y, Carass A, Prince JL, Resnick SM. Longitudinal analysis of regional cerebellum volumes during normal aging. *NeuroImage*. 2020;220:117062. doi:10.1016/j.neuroimage.2020.117062
24. Bede P, Chipika RH, Finegan E, et al. Brainstem pathology in amyotrophic lateral sclerosis and primary lateral sclerosis: A longitudinal neuroimaging study. *NeuroImage Clin*. 2019;24:102054. doi:10.1016/j.nicl.2019.102054
25. Querin G, El Mendili MM, Lenglet T, et al. Spinal cord multi-parametric magnetic resonance imaging for survival prediction in amyotrophic lateral sclerosis. *Eur J Neurol*. 2017;24(8):1040–1046. doi:10.1111/ene.13329
26. Whitwell JL, Weigand SD, Boeve BF, et al. Neuroimaging signatures of frontotemporal dementia genetics: C9ORF72, tau, progranulin and sporadics. *Brain*. 2012;135(3):794–806. doi:10.1093/brain/aws001
27. Consonni M, Dalla Bella E, Nigri A, et al. Cognitive syndromes and C9orf72 mutation are not related to cerebellar degeneration in amyotrophic lateral sclerosis. *Front Neurosci*. 2019;13:440. doi:10.3389/fnins.2019.00440
28. Bharti K, Khan M, Beaulieu C, et al. Involvement of the dentate nucleus in the pathophysiology of amyotrophic lateral sclerosis: A multi-center and multi-modal neuroimaging study. *NeuroImage Clin*. 2020;28:102385. doi:10.1016/j.nicl.2020.102385
29. Schönecker S, Neuhofer C, Otto M, et al. Atrophy in the thalamus but not cerebellum is specific for C9orf72 FTD and ALS patients: An Atlas-based volumetric MRI study. *Front Aging Neurosci*. 2018;10:45. doi:10.3389/fnagi.2018.00045
30. Kim HJ, Oh SI, De Leon M, et al. Structural explanation of poor prognosis of amyotrophic lateral sclerosis in the non-demented state. *Eur J Neurol*. 2017;24(1):122–129. doi:10.1111/ene.13163
31. Shen D, Hou B, Xu Y, et al. Brain structural and perfusion signature of amyotrophic lateral sclerosis with varying levels of cognitive deficit. *Front Neurol*. 2018;9:364. doi:10.3389/fneur.2018.00364
32. Cosottini M, Giannelli M, Siciliano G, et al. Diffusion-tensor MR imaging of corticospinal tract in amyotrophic lateral sclerosis and progressive muscular atrophy. *Radiology*. 2005;237(1):258–264. doi:10.1148/radiol.2371041506
33. Li J, Pan P, Song W, Huang R, Chen K, Shang H. A meta-analysis of diffusion tensor imaging studies in amyotrophic lateral sclerosis. *Neurobiol Aging*. 2012;33(8):1833–1838. doi:10.1016/j.neurobiolaging.2011.04.007
34. Verstraete E, Polders DL, Mandl RCW, et al. Multimodal tract-based analysis in ALS patients at 7T: A specific white matter profile? *Amyotroph Lateral Scler Frontotemporal Degener*. 2014;15(1–2):84–92. doi:10.3109/21678421.2013.844168
35. Zhang F, Chen G, He M, et al. Altered white matter microarchitecture in amyotrophic lateral sclerosis: A voxel-based meta-analysis of diffusion tensor imaging. *NeuroImage Clin*. 2018;19:122–129. doi:10.1016/j.nicl.2018.04.005
36. Menke RAL, Proudfoot M, Wu J, et al. Increased functional connectivity common to symptomatic amyotrophic lateral sclerosis and those at genetic risk. *J Neurol Neurosurg Psychiatry*. 2016;87(6):580–588. doi:10.1136/jnnp-2015-311945
37. De Marchi F, Stecco A, Falaschi Z, et al. Detection of white matter ultrastructural changes for amyotrophic lateral sclerosis characterization: A diagnostic study from Dti-derived data. *Brain Sci*. 2020;10(12):996. doi:10.3390/brainsci10120996
38. Budrewicz S, Szewczyk P, Bładowska J, et al. The possible meaning of fractional anisotropy measurement of the cervical spinal cord in correct diagnosis of amyotrophic lateral sclerosis. *Neurol Sci*. 2016;37(3):417–421. doi:10.1007/s10072-015-2418-4
39. Qiu T, Zhang Y, Tang X, et al. Precentral degeneration and cerebellar compensation in amyotrophic lateral sclerosis: A multimodal MRI analysis. *Hum Brain Mapp*. 2019;40(12):3464–3474. doi:10.1002/hbm.24609
40. Tu S, Menke RAL, Talbot K, Kiernan MC, Turner MR. Cerebellar tract alterations in PLS and ALS. *Amyotroph Lateral Scler Frontotemporal Degener*. 2019;20(3–4):281–284. doi:10.1080/21678421.2018.1562554
41. Keil C, Prell T, Peschel T, Hartung V, Dengler R, Grosskreutz J. Longitudinal diffusion tensor imaging in amyotrophic lateral sclerosis. *BMC Neurosci*. 2012;13(1):141. doi:10.1186/1471-2202-13-141
42. Barry RL, Babu S, Anteraper SA, et al. Ultra-high field (7T) functional magnetic resonance imaging in amyotrophic lateral sclerosis: A pilot study. *NeuroImage Clin*. 2021;30:102648. doi:10.1016/j.nicl.2021.102648
43. Bede P, Bokde ALW, Byrne S, et al. Multiparametric MRI study of ALS stratified for the C9orf72 genotype. *Neurology*. 2013;81(4):361–369. doi:10.1212/WNL.0b013e31829c5eee
44. DeJesus-Hernandez M, Mackenzie IR, Boeve BF, et al. Expanded GGGGCC hexanucleotide repeat in noncoding region of C9ORF72 causes chromosome 9p-linked FTD and ALS. *Neuron*. 2011;72(2):245–256. doi:10.1016/j.neuron.2011.09.011